AIAA JOURNAL
Vol. 40, No. 4, April 2002

Mixer–Ejector Wall Pressure and Temperature Measurements Based on Photoluminescence

Ray R. Taghavi*
University of Kansas, Lawrence, Kansas 66045
Ganesh Raman†
Illinois Institute of Technology, Chicago, Illinois 60616-3793
and
Timothy J. Bencic‡
NASA John H. Glenn Research Center at Lewis Field, Cleveland, Ohio 44135

Ejector side-wall pressure distribution is a key indicator of supersonic jet-mixer–ejector performance. When documenting pressure patterns on an ejector wall using pressure-sensitive paint (PSP), one has to consider temperature variations caused by the supersonic jet flow within the ejector because these can cause significant local errors in the PSP results. If the temperature sensitivity of PSP is not corrected for in complex internal supersonic flows, large localized errors could contaminate the results. In the present work, temperature-sensitive paint maps the temperature distribution on the ejector wall and corrects PSP results point-by-point for temperature sensitivity. The experiments were conducted on multijet supersonic mixer–ejector configurations with straight, convergent (6-deg), and divergent (6-deg) side walls. A comparison of corrected and uncorrected PSP readings shows that at $M_j = 1.55$, the error with respect to true data from static pressure ports can be reduced from 4.98 to 2.84% for the case of a simple ejector with parallel walls. For the complex 6-deg convergent ejector at $M_j = 1.39$, the error reduces by almost an order of magnitude (from 20.83 to 2.66%). Our results indicate that the use of this correction technique can significantly reduce PSP errors in complex internal supersonic flow situations.

I. Introduction

THE future High-Speed Civil Transports require properly designed mixer–ejector nozzles for noise suppression and thrust augmentation. In recent papers, Taghavi and Raman,[1] Raman and Taghavi,[2] and Taghavi et al.[3] showed that the ejector wall pressure in complex multijet supersonic jet mixer–ejector nozzles is a very good indicator of ejector performance characteristics such as exit mean flow uniformity, flow separation, pumping, and thrust augmentation. The pressure-sensitive paint (PSP) and temperature-sensitive paint (TSP) techniques have proven ideal for wall pressure and temperature measurements. The PSP technique has already been used to obtain global surface pressure measurements in wind tunnels, flow facilities, and flight tests.[3–13] Compared to conventional pressure measurements using discrete pressure taps, the PSP technique provides extensive surface pressure information in a shorter time and at a lower cost. Many researchers[14–17] have emphasized the importance of correcting for PSP temperature sensitivity, which is caused by at least three factors[17]: 1) The luminescence process itself could depend on temperature. 2) The solubility of oxygen in the paint matrix could depend on temperature (especially when the luminophore is dissolved in a silicone polymer matrix). 3) The quenching reaction could be temperature dependent. Thus, as reported earlier,[14–17] and as is clearly evident from the results of this investigation, we must correct the PSP data for temperature to obtain a valid analysis of ejector performance. For the present set of experiments we selected a complex internal flow situation produced by operating a supersonic multijet mixer-ejector nozzle with Plexiglas™ walls. TSP was first applied to map the temperature on the ejector's side wall. PSP was subsequently applied, and the results were corrected point-by-point for temperature sensitivity. We demonstrate that this correction method can significantly reduce PSP errors in supersonic jet-mixer–ejector applications.

Received 26 August 1998; revision received 13 July 2001; accepted for publication 19 July 2001.

*Professor, Department of Aerospace Engineering. Associate Fellow AIAA.
†Associate Chair for Aerospace Engineering and Associate Professor, Mechanical and Aerospace Engineering Department. Associate Fellow AIAA.
‡Aerospace Engineer, Optical Instrumentation Technology Branch.

II. Experimental Facility and Instrumentation

The experiments were carried out in the NASA John H. Glenn Research Center Supersonic Jet Facility. The detailed description of the facility can be found in Refs. 1 and 2 and will be briefly presented here. A schematic and photograph of the facility are shown in Figs. 1 and 2, respectively. The plenum tank was supplied with compressed air at pressures up to 875 kPa (125 psig) at 26.7°C (80°F). After passing through a filter, acoustic treatment section, and two 50-mesh screens, the primary air emerged from four convergent rectangular nozzles (6.9 × 34.5 mm) (0.27 × 1.36 in.), into the inlet area of the adjustable area rectangular ejector. An automatic feedback control system was used to maintain constant air supply conditions. The control system could restrict pressure variations during each run to within 0.2%. Raman and Taghavi[2] showed that both acoustic and flowfield data could be reproduced accurately from day to day. The internozzle spacing was $s/h = 4.6$ with s being the center-to-center spacing of the adjacent nozzles and h the narrow dimension of the nozzles. The primary jet fully expanded Mach number M_j for these experiments ranged from 0.8 to 1.55. The fully expanded Mach number is defined for an underexpanded nozzle as the Mach number calculated by using the isentropic equation

$$P_0/P = \{1 + [(\gamma - 1)/2]M^2\}^{\gamma/(\gamma-1)}$$

in which P_0 and P are the jet's stagnation pressure and the nozzle back pressure, respectively. This is the Mach number that the jet would theoretically attain on isentropic expansion.

The adjustable area rectangular ejector shown in Fig. 2a was originally designed for the experiments of Rice.[18] The ejector area ratio (ejector exit area divided by the total nozzle exit area) for these experiments was 4.6. The ejector convergence/divergence angle could be adjusted by using tapered spacers. In these experiments, 6-deg convergent and divergent angles were studied. The side walls were constructed from Plexiglas to allow for flow visualization.

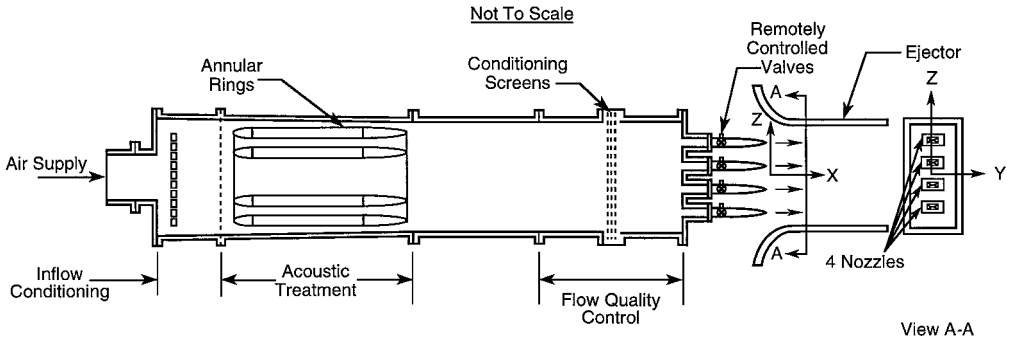

Fig. 1 Schematic of supersonic jet flow facility.

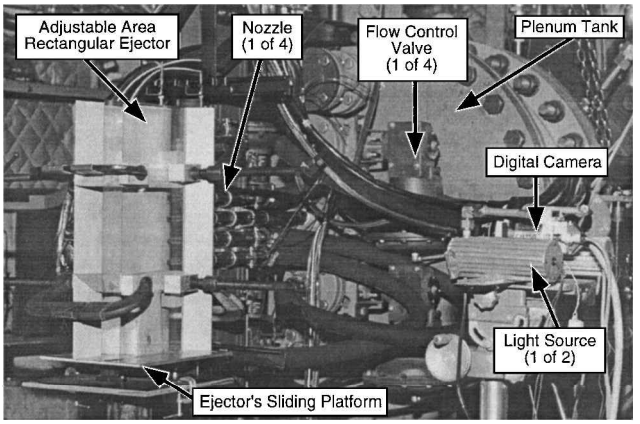

a) Pressure and temperature paint setup

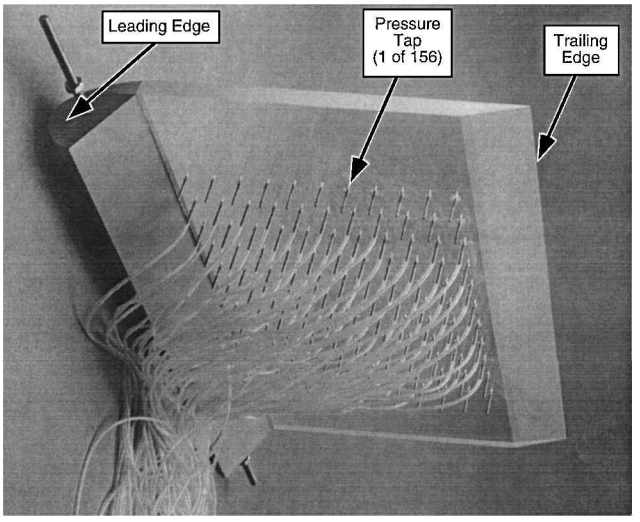

b) Ejector side wall with pressure taps and thermocouples

Fig. 2 Photograph of experimental apparatus.

An extra side wall was fabricated for PSP/TSP experiments as shown in Fig. 2b. This side wall was instrumented with 115 static taps and 41 thermocouples, connected to the electronic scanning pressure modules to measure the surface static pressure and temperature distributions for calibration of and comparison with the PSP/TSP data. The pressure taps/thermocouples extended from 1.12 cm (0.44 in.) downstream of the throat line [6.20 cm (2.44 in.) from the leading edge] to 5.72 cm (2.25 in.) upstream of the trailing edge. Some pressure taps and thermocouples were also provided to measure the pressure and temperature distributions on the leading-edge area of the ejector.

III. PSP/TSP Setup and Data Acquisition

Because a detailed description of the PSP/TSP techniques exists in the literature,[3–17] we will not reiterate it here. The paints used for the experiments described in this paper were PSP [McDonnell Douglas Aerospace (MDA) PF2B] (Refs. 5–7) and MDA-TSP obtained from MDA (now Boeing Aircraft Company). A glossy white base coat (MDA WAL-2) was applied to the model before the application of the PSP. TSP is a single-coat paint and was applied directly to the model. Note that we do not correct for the effect of the temperature drop across the PSP primer layer in this paper. The PSP and TSP runs were conducted on different days. However, the automatic feedback control system maintained constant air supply conditions leading to reproducible results for surface pressures, acoustics, and flowfields.[2]

Figure 2 depicts the imaging hardware of the PSP/TSP data acquisition system used for these experiments. Excitation of the probe molecules was accomplished by two filtered, 75-W, 12-V tungsten halogen lamps with integral reflectors. The light wavelength required for excitation was in the 430–470-nm (1.41×10^{-6}–1.54×10^{-6} ft) bandwidth. This was accomplished by selective band filtering of the illumination lamps. Interference filters were used for passing light in the excitation band and reflecting unwanted light outside the band. Because the interference filters reflect the light that is not passed, cooling must be provided to carry away the heat from the light housings. Cooling for the light housings was provided by regulated service air at 45 psig. Also, the effect of photolytic decomposition of PSP/TSP was made insignificant by limiting the power of the PSP/TSP excitation source.

The camera used in these experiments was a cooled scientific grade imager capable of 14-bit resolution (approximately 16,000 intensity graduations) with a full well capacity of 350 kiloelectrons. It had a spatial resolution of 512×512 pixels. The TSP and PSP measurements were shot-noise limited. In the acquisition of the steady-state data, an eight-frame average was performed to increase the signal-to-noise ratio. The camera was optically filtered to allow only the light from luminescence to be incident on the imager (detection pass band was 530–650 nm) (1.74×10^{-6}–2.13×10^{-6} ft). This was accomplished by positioning a bandpass filter in front of the camera lens.

The acquired images were processed using an intensity-based data reduction technique for both TSP and PSP. This technique requires the two images, a wind-off I_{ref} reference image and a wind-on I_{data} data image to determine the magnitude of the measurements. The simple two-dimensional movement of the ejector was corrected using the static ports as registration marks between the wind-off and wind-on images. Nonuniformities in paint application and excitation lighting were corrected by taking the ratio of I_{ref} by I_{data}. An a priori or batch TSP calibration that depended on the composition of the paint was applied to the ratio image and an in situ calibration using data from all thermocouples was used to correct the initial calibration. The difference between the a priori calibration and the final in situ calibrated images revealed a 1–2.5% slope change for the PSP and a 0.5–1% change for the TSP over the pressure and temperature ranges encountered. The a priori TSP temperature calibration is initially used to convert the temperature intensity ratio image to a quantitative temperature image. After the application of the a priori calibration to determine a rough scale, the thermocouples on the test article were used to generate an in situ calibration and produce a more accurate measurement. This method contains an extra step that typically is not performed, that is, the a priori calibration, but in performing this step, the shelf life and the response of the paints can be tracked to see if any long-term deterioration of the paint occurs.

The PSP intensity ratio needed a temperature correction because the surface temperature varied relative to the jet location. A temperature correction was applied to the PSP intensity ratio using the TSP images acquired during the experiment. A temperature correction image was generated using $T_{\text{cor}} = 1 - a\Delta T$, where $a = 0.004758$ and ΔT is the change in temperature from the wind-off images. Note that the constant a was determined by the paint manufacturer (MDA) for the paint used in this work. The calibration of the PSP images followed in a similar manner to the TSP images and the PSP intensity ratio ($I_{\text{ref}}/I_{\text{data}}$) corrected by multiplying by T_{cor}. The basis for this temperature correction method appears in Ref. 19 and was checked in the cavity flow experiment of Raman et al.[20]

IV. Results

The ejector pumping (ejector exit mass flow minus primary jet mass flow per primary jet mass flow) was calculated by integration of the flowfield data over the entire ejector exit cross section for $M_j = 1.39$. The primary jet mass flow rate was estimated using isentropic relationships. The ejector pumping was 0.49, 0.41, and 0.78 for straight-walled, convergent, and divergent ejectors, respectively. These data clearly reveal that increasing the ejector side-wall convergence angle from 0 (straight walls) to 6 deg results in a 16% reduction in ejector pumping. On the other hand, diverging the ejector side walls from 0 to 6 deg results in a 59% increase in ejector pumping. This trend reverses at higher divergence angles, possibly because of flow separation from the ejector side walls.

The PSP and TSP images of the ejector's side-wall at $M_j = 1.39$ for parallel, 6-deg divergent, and 6-deg convergent side-wall configurations are shown in Fig. 3. To enhance the details, different color bars were selected for each case. These data are represented as surface pressure coefficient C_p and surface temperature coefficient C_T contours. C_p is defined as $(P - P_{\text{amb}})/P_{\text{amb}}$, in which P and P_{amb} are the local surface and ambient pressures, respectively. C_T is defined as $(T - T_{\text{amb}})/T_{\text{amb}}$, in which T and T_{amb} are the local surface and ambient temperatures, respectively. All of the PSP images are corrected for temperature. The vertical stripes are due to the light refraction from the corner of the tapered trailing edge of the ejector side wall.

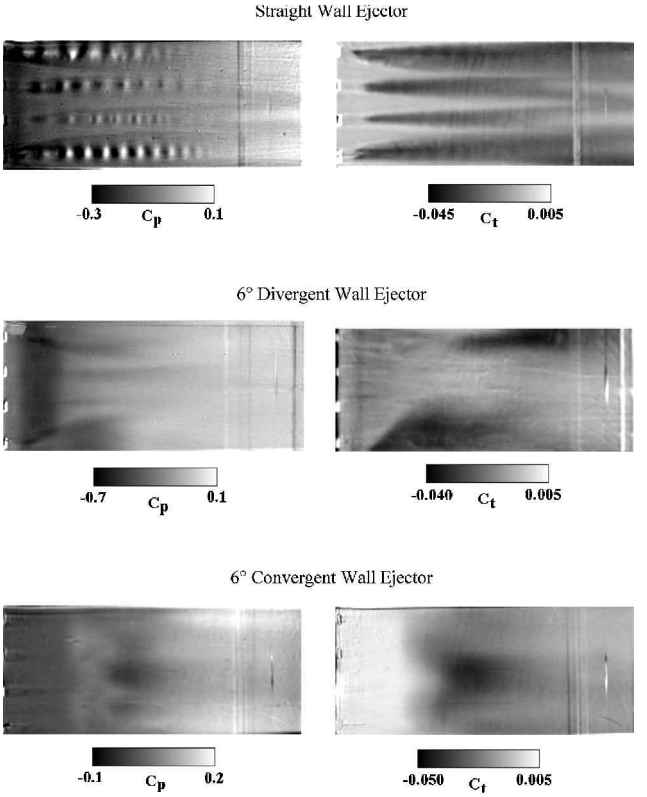

Fig. 3 PSP (left) and TSP (right) images of the ejector side wall at different convergence/divergence angles ($M_j = 1.39$).

The PSP and TSP images clearly reveal the complex nature of side-wall pressure and temperature patterns that are indicators of the mixing processes occurring within the ejector. In Fig. 3, flow is from left to right, and the left edge of the image corresponds to the throat of the ejector (location of the primary nozzle exits). A low-pressure and high-temperature region is visible in the suction (throat) region of the ejector. For the case of ejector with straight walls, the shock-cell structures of the primary jets are clearly visible from the PSP

Table 1 Temperature statistics on the ejector wall

M_j	ΔT_{min}	ΔT_{max}	ΔT_{ave}	Standard deviation
Straight wall ejector configuration				
0.92	−14.778	4.590	−6.269	2.630
0.98	−16.112	1.366	−6.776	2.774
1.04	−17.232	1.687	−7.293	3.096
1.17	−19.846	4.108	−8.856	4.535
1.39	−18.833	0.629	−9.480	4.048
1.55	−26.088	0.505	−12.404	4.915
6-deg convergent ejector configuration				
0.92	−6.226	0.864	−2.218	1.567
0.98	−10.126	1.308	−4.083	2.462
1.04	−9.139	0.696	−3.350	2.437
1.17	−10.451	1.602	−4.887	2.872
1.39	−25.779	3.099	−9.811	6.765
1.55	−15.616	2.397	−5.383	4.167
6-deg divergent ejector configuration				
0.92	−13.87	0.442	−4.141	2.505
0.98	−15.002	0.048	−4.715	2.586
1.04	−17.381	−0.554	−5.522	2.877
1.17	−18.971	−2.012	−7.021	3.390
1.39	−19.889	−1.434	−8.291	3.749
1.55	−20.684	0.295	−8.675	3.969

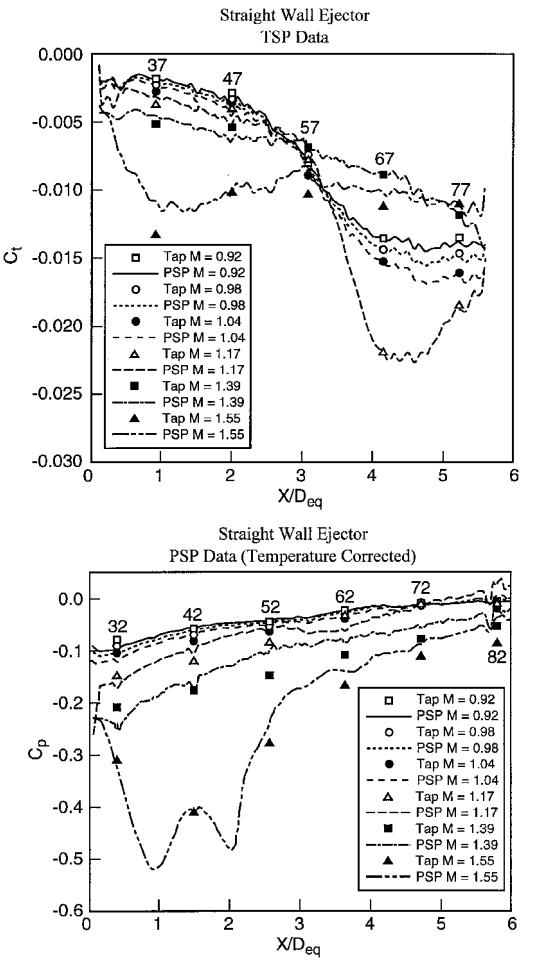

Fig. 4 Comparison of the TSP and temperature-corrected PSP results with thermocouple/pressure tap data along the centerline of the ejector side wall (straight-wall ejector).

Table 2 Estimate of the maximum error for a single pressure tap in the PSP measurement with and without temperature correction

M_j	Largest error tap number	Tap C_p	Uncorrected image C_p	Corrected image C_p	Difference uncorrected, %	Difference corrected, %
			Straight wall ejector configuration			
0.92	78	−0.001	0.017	0.003	1.729	0.341
0.98	48	−0.053	−0.074	−0.057	2.027	0.388
1.04	48	−0.062	−0.092	−0.070	2.993	0.743
1.17	58	−0.039	−0.109	−0.074	6.952	3.462
1.39	52	−0.149	−0.082	−0.109	6.729	4.046
1.55	52	−0.279	−0.200	−0.235	7.915	4.411
			6-deg convergent ejector configuration			
0.92	52	−0.005	0.000	−0.003	0.493	0.184
0.98	72	0.050	0.042	0.044	0.739	0.552
1.04	72	0.055	0.047	0.049	0.797	0.582
1.17	56	0.021	0.002	0.023	1.977	0.186
1.39	62	0.077	−0.407	0.014	48.43	6.285
1.55	56	−0.013	0.031	0.019	4.44	3.198
			6-deg divergent ejector configuration			
0.92	48	−0.124	−0.089	−0.096	3.477	2.781
0.98	76	−0.031	0.018	−0.009	4.862	2.229
1.04	48	−0.135	−0.197	−0.190	6.169	5.489
1.17	48	−0.200	−0.312	−0.304	11.205	10.420
1.39	48	−0.283	−0.418	−0.372	13.544	8.890
1.55	42	−0.428	−0.463	−0.457	3.471	2.891

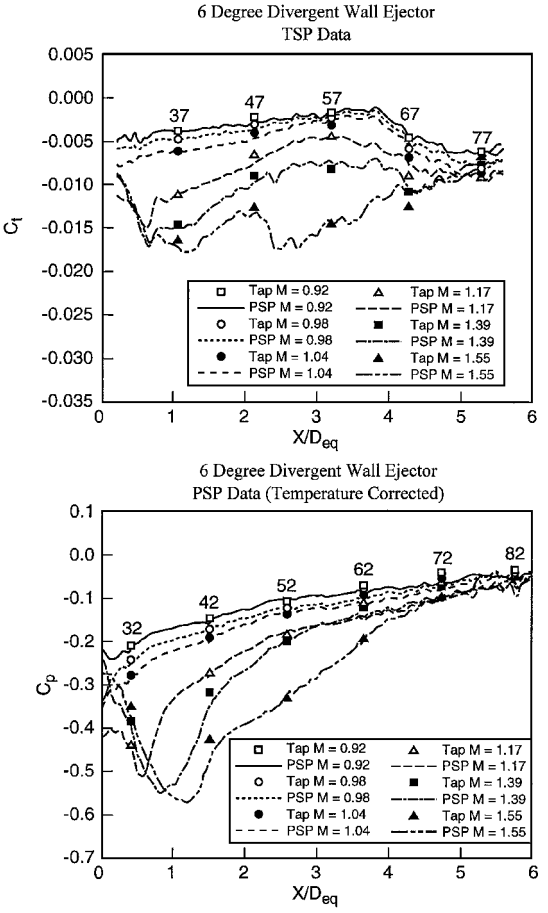

Fig. 5 Comparison of the TSP and temperature-corrected PSP results with thermocouple/pressure tap data along the centerline of the ejector side wall (6-deg divergent wall ejector).

image. For the same case, the higher mixing of the outside primary jets (top and bottom) compared to the middle primary jets is shown in the TSP image. Flow separation patterns from the ejector's side wall for the 6-deg divergence case are shown in the PSP image (light gray). Isolated bubbles of separated flow (dark spots of low pressure and low temperature in the middle) are visible for the convergent-wall PSP and TSP images.

Pressure and temperature distributions along the centerline of the ejector side wall, obtained from PSP and TSP techniques over the entire range of primary jet Mach numbers and their comparison with pressure tap and thermocouple data, are shown in Figs. 4–6. The numbers on the plots are the locations of specific static taps and thermocouples along the centerline of the ejector's side wall. Excellent agreement between the TSP data and thermocouples, as well as the temperature-corrected PSP and pressure-tap data, is observed in Figs. 4–6. The uncertainty of the thermocouple and pressure transducer measurements were ±1.11°C (±2°F) and ±0.15 kPa (±0.02 psi), respectively.

Table 3 PSP rms errors for the entire ejector surface for all pressure taps with and without temperature corrections

M_j	RMS error without temperature correction	RMS error with temperature correction
	Straight wall ejector configuration	
0.92	1.53	0.62
0.98	1.97	0.90
1.04	2.16	1.03
1.17	5.31	2.53
1.39	3.85	2.09
1.55	4.98	2.84
	6-deg convergent ejector configuration	
0.92	0.32	0.46
0.98	0.63	0.64
1.04	0.52	0.54
1.17	1.20	0.46
1.39	20.83	2.66
1.55	2.39	1.83
	6-deg divergent ejector configuration	
0.92	2.19	1.79
0.98	2.35	1.91
1.04	2.58	2.39
1.17	4.46	3.90
1.39	4.79	4.22
1.55	1.61	1.81

The effects of temperature correction will be described in the following paragraphs. Figure 7a shows the temperature distribution on the ejector wall for the case of straight-walled ejector at $M_j = 1.55$. Superimposed on the temperature map are the static pressure port locations denoted by numbers. The ports were numbered from 1 to 115, and the ports used for the present calibration are shown in Fig. 7a. Figure 7b shows a plot of image pressure vs static tap pressure. Ideal behavior is represented by the diagonal line. Values of both image and true pressure with and without temperature correction are plotted. It is clear that the temperature correction of the PSP data resulted in getting them closer to the diagonal. Results from a detailed error analysis are presented in Tables 1–3 for the entire

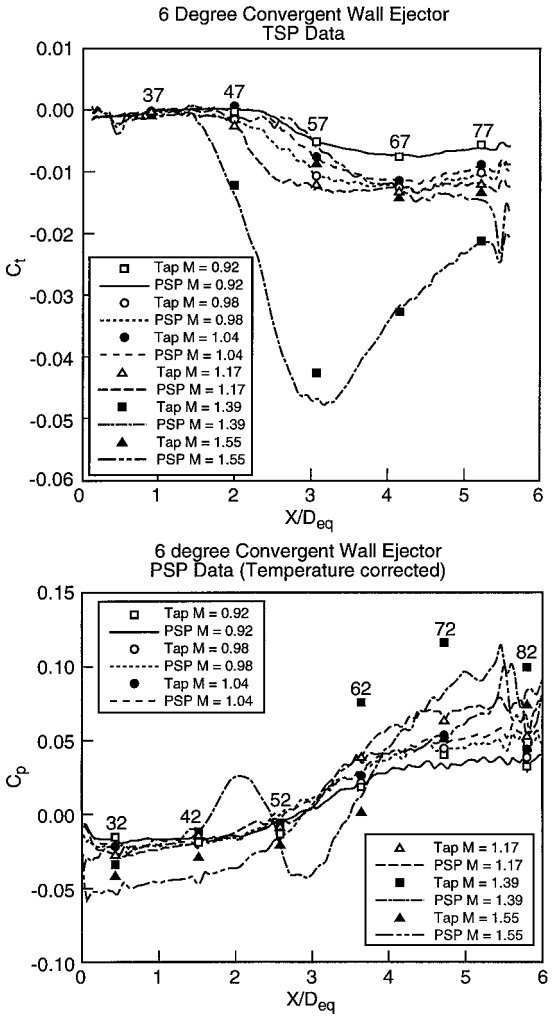

Fig. 6 Comparison of the TSP and temperature-corrected PSP results with thermocouple/pressure tap data along the centerline of the ejector side wall (6-deg convergent wall ejector).

range of Mach numbers. Table 1 provides temperature statistics on the ejector wall. Note that $\Delta T_{\min}$ and $\Delta T_{\max}$ represent the minimum and maximum temperature deviations on the ejector side wall from the ambient temperature, and negative values represent temperatures below ambient. The ΔT_{ave} is the average value of temperature deviations from all thermocouples on the ejector wall; therefore, it is not the midpoint between $\Delta T_{\min}$ and $\Delta T_{\max}$. The data of Table 2 indicate the effect of PSP correction for temperature dependence on the maximum error on the ejector wall over the entire M_j range for single pressure taps. Note that an improvement (with temperature correction) in the maximum error is observed at all values of M_j. The pressure tap location (number) where the maximum error occurs is given in the last column (see Fig. 7a for tap locations). Finally, the rms errors for the entire ejector surface (all pressure taps) with and without temperature correction are shown in Table 3. The rms error was obtained by taking the difference between PSP (corrected and uncorrected) and true static pressure tap values at each of the pressure tap locations and calculating the root mean square (expressed as a percent of the true value). This represents an integral measure of the error on the ejector wall for various cases. From the data, it is clear that it is not the maximum or minimum temperature that determines the magnitude of error (see Table 1) but the temperature gradient (see Table 2) in the region of the pressure tap. In the present case the maximum percent error occurred at port 52, which is in a region of strong temperature gradient. Tables 1 and 2 present a summary of such data for all cases considered in this study. A general conclusion from these data is that the maximum and minimum temperatures do not influence the PSP error.

Finally, we analyze the importance of the temperature correction for two complex flow configurations. One configuration chosen

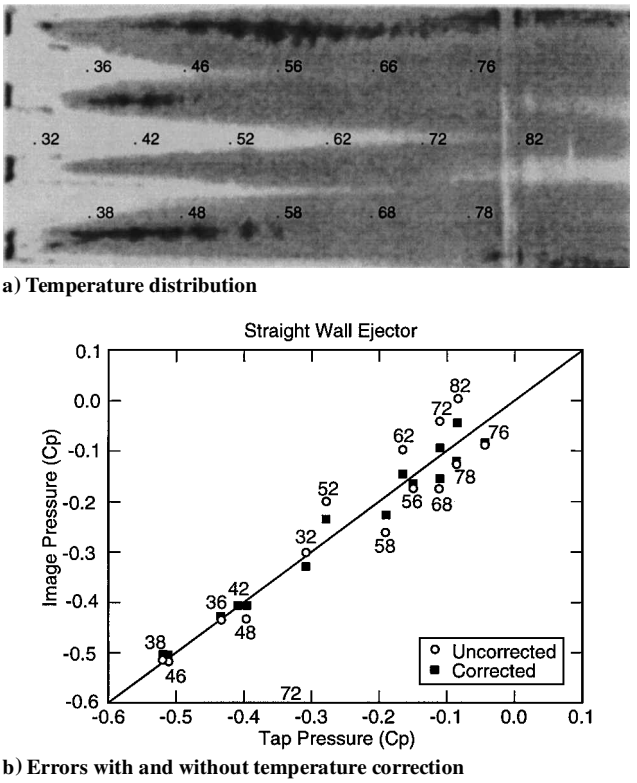

Fig. 7 Relationship between the temperature distribution and errors with and without temperature correction; ejector with straight wall, $M_j = 1.55$.

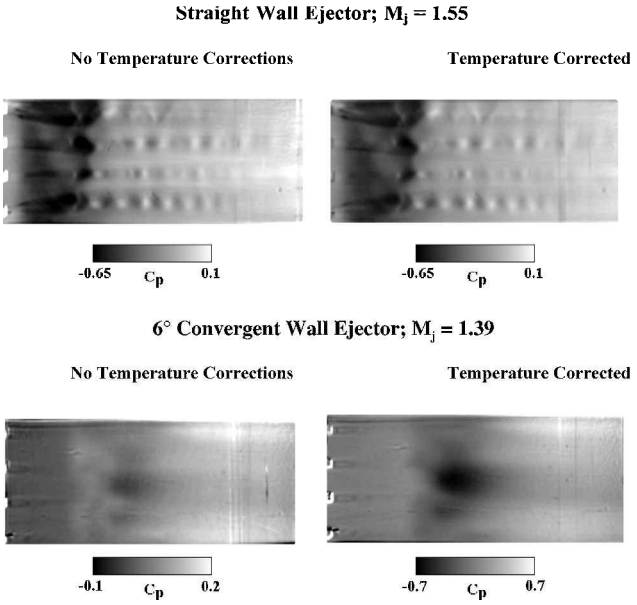

Fig. 8 Comparison of PSP images with and without temperature correction.

was an ejector with parallel walls with the primary jets operating at $M_j = 1.55$ and the other was an ejector with 6-deg convergent walls at $M_j = 1.39$. Figure 8 compares PSP images with and without temperature correction for the two cases. For the parallel-walled ejector, the temperature correction only produced a small change in the PSP results whereas the change was profound for the convergent-walled ejector. This dramatic change is illustrated in Fig. 9 using data along one axial line on the ejector wall. Despite the complexity of the PSP pattern in Fig. 9a (also see Fig. 8), the errors are moderate. In contrast, for Fig. 9b very large errors arise due to impingement of the jet flow on the ejector wall. This impingement, which occurs around $x/D_{\text{eq}} = 3$, produces a very complex temperature distribution, thus

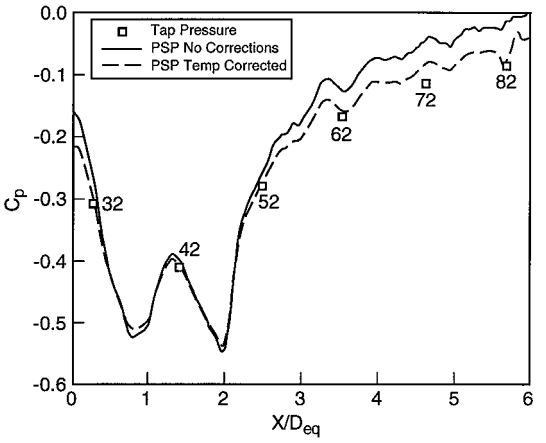

a) Straight-wall ejector, $M_j = 1.55$

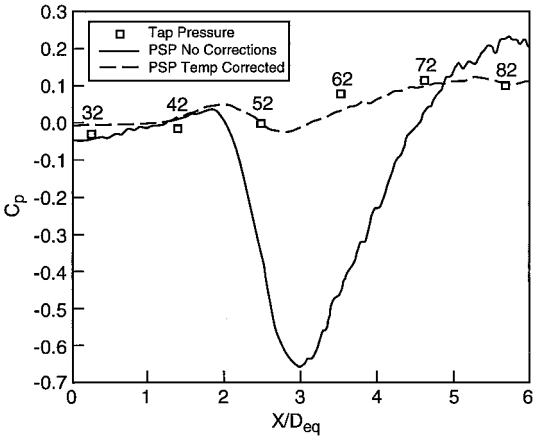

b) 6-deg convergent ejector, $M_j = 1.39$

Fig. 9 Effects of temperature correction on PSP measurements errors.

contaminating the PSP results. When we correct for the temperature sensitivity of the PSP, the errors reduce dramatically. The rms error (an integral measure of the error on the ejector wall) is given in Table 3 with and without temperature correction for three ejector configurations operated at various primary jet Mach numbers M_j from 0.92 to 1.55. Note from Table 3 that for the case depicted in Fig. 9a the error reduces from 4.98 to 2.84% when corrected for temperature. A more dramatic change is seen for the case depicted in Fig. 9b, where the error reduces from 20.83 to 2.66%. Thus, our data are successful in proving that the temperature correction can significantly reduce PSP errors in complex ejector flow configurations. Note that complex interactions in the ejector, including flow impingement on ejector walls, cause the flow patterns to be entirely different at various Mach numbers.

V. Conclusions

Ejector side-wall pressure measurements made by using the PSP technique were corrected for temperature sensitivity by the use of TSP. A complex flow situation involving a supersonic jet-mixer–ejector nozzle was chosen for these tests. Ejectors with parallel, convergent (6-deg), and divergent (6-deg) side walls were used at primary jet Mach numbers of up to 1.55. It was clearly demonstrated that the magnitude of the correction depended on the complexity of the flow situation. For the case of a simple ejector with parallel walls at $M_j = 1.55$, our correction reduced the error from 4.98 to 2.84%. For the complex case of a 6-deg convergent ejector at $M_j = 1.39$, which involved local regions where the jets impinged on the ejector wall, our correction reduced the error by almost an order of magnitude from 20.83 to 2.66%. It is hoped that the use of this correction technique would allow for accurate ejector wall pressure data that would be useful for evaluating ejector performance.

Acknowledgments

This research was conducted under Grant NAG3-1805 from NASA John H. Glenn Research Center. The authors thank Khairul Zaman of NASA John H. Glenn Research Center for his support and technical input and Edward J. Rice for the design of the ejector and multijet facility. The technical support of Richard Brokopp and James Nichols (mechanical) and James Little (electronics) is highly appreciated.

References

[1]Taghavi, R., and Raman, G., "Flow Characteristics of a Rectangular Multielement Supersonic Mixer–Ejector," *Journal of Propulsion and Power*, Vol. 12, No. 5, 1996, pp. 1004–1107.

[2]Raman, G., and Taghavi, R., "Aeroacoustics Characteristics of a Rectangular Multi-Element Supersonic Jet Mixer-Ejector Nozzle," *Journal of Sound and Vibration*, Vol. 207, No. 2, 1997, pp. 227–248.

[3]Taghavi, R., Raman, G., and Bencic, T., "Visualization of Ejector Wall Pressure Using Pressure Sensitive Paint," American Society of Mechanical Engineers, ASME Paper FEDSM97-3236, June 1997.

[4]Kavandi, J., Callis, J., Gouterman, M., Khalil, G., Wright, D., Green, E., Bvens, D., and McLachlan, B., "Luminescence Barometry in Wind Tunnels," *Review of Scientific Instruments*, Vol. 61, No. 11, 1990, pp. 3340–3347.

[5]Morris, M. J., Benne, M. E., Crites, R. C., Donovan, J. F., "Aerodynamic Measurements Based on Photoluminescence," AIAA Paper 93-0175, Jan. 1993.

[6]Morris, M. J., Donovan, J. F., Kegelman, J. T., Schwab, S. D., Levy, R. L., and Crites, R. C., "Aerodynamic Applications of Pressure Sensitive Paint," AIAA Paper 92-0264, Jan. 1992.

[7]Morris, M. J., and Donovan, J. F., "Application of Pressure- and Temperature-Sensitive Paint to High-Speed Flows," AIAA Paper 94-2231, June 1994.

[8]McLachlan, B. G., Kavandi, J., Gouterman, M., Green, D., Khalil, G., and Burns, D., "A Surface Pressure Field Mapping Using Luminescent Coatings," *Experiments in Fluids*, Vol. 14, 1993, pp. 33–41.

[9]Bencic, T. J., "Experiences Using Pressure Sensitive Paint in NASA Lewis Research Center Propulsion Test Facilities," AIAA Paper 95-2831, July 1995.

[10]Bencic, T. J., "Rotating Pressure and Temperature Measurements on Scale-Model Fans Using Luminescent Paints," AIAA Paper 98-3452, July 1998.

[11]Peterson, J. I., and Fitgerald, V. F., "New Technique of Surface Flow Visualization Based on Oxygen Quenching of Fluorescence," *Review of Scientific Instruments*, Vol. 51, No. 5, 1980, pp. 670, 671.

[12]Cler, D., Lamb, M., Farokhi, S., Taghavi, R., and Hazlewood, R., "Application of Pressure-Sensitive Paint in Supersonic Nozzle Research," *Journal of Aircraft*, Vol. 33, No. 6, 1996, pp. 1109–1114.

[13]Lepicovsky, J., Bencic, T. C., and Bruckner, R. J., "Application of Pressure-Sensitive Paint to Confined Flow at Mach Number 2.5," AIAA Paper 97-3214, July 1997.

[14]Liu, T., Campbell, B. T., and Sullivan, J. P., "Thermal Paints for Shock/Boundary-Layer Interaction in Inlet Flows," AIAA Paper 92-3626, July 1992.

[15]Woodmansee, M. A., and Dutton, J. C., "Treating Temperature-Sensitivity Effects of Pressure-Sensitive Paint," *Experiments in Fluids*, Vol. 24, 1998, pp. 163–174.

[16]Schanze, K. S., Carroll, B. F., Korotkevitch, S., and Morris, M., "Temperature Dependence of Pressure Sensitive Paints," *AIAA Journal*, Vol. 35, No. 2, 1997, pp. 306–310.

[17]Oglesby, D. M., Upchurch, B. T., Leighty, B. D., Simmons, K. A., and Demandante, C. G., "Pressure Sensitive Paint with Internal Temperature Sensing Luminophore," *Proceedings of the 42nd International Instrumentation Symposium*, Instrumentation, Systems, and Automation Society, Research Triangle Park, NC, 1996, pp. 205–224.

[18]Rice, E. J., "Jet Mixer Noise Suppressor Using Acoustic Feedback," U.S. Patents 5,325,661 and 5,392,597, 1995.

[19]Bencic, T. J., "Pressure-Sensitive Paint Measurements on Surfaces with Non-Uniform Temperature," *Proceedings of the 45th International Instrumentation Symposium*, Power Engineering Books, St. Albert, AB, Canada, 1999, pp. 355–364.

[20]Raman, G., Envia, E., and Bencic, T. J., "Tone Noise and Near-Field Pressure Produced by Jet–Cavity Interaction," AIAA Paper 99-0604, 1999.

R. P. Lucht
Associate Editor